Journal of Chromatography A, 1216 (2009) 5962–5967

Contents lists available at ScienceDirect

Journal of Chromatography A

journal homepage: www.elsevier.com/locate/chroma

# Size-fractionation of silver nanoparticles using ion-pair extraction in a counter-current chromatograph

Ching-Wei Shen, Tiing Yu*

*Department of Applied Chemistry, National Chiao Tung University, Hsinchu 30050, Taiwan*

ARTICLE INFO

*Article history:*
Received 25 January 2009
Received in revised form 28 May 2009
Accepted 2 June 2009
Available online 6 June 2009

*Keywords:*
Counter-current chromatography
Silver nanoparticles
Size separation
Ion-pair
Phase transfer
Step-gradient extraction

ABSTRACT

Size separation of silver nanoparticles was investigated in counter-current chromatography (CCC) based on a unique step-gradient extraction process. Carboxylate anions were modified on silver nanoparticles to produce water-dispersible nanoparticles. The aqueous nanoparticles were readily transferred to the organic phase (toluene/hexane = 1:1, v/v) together with the phase transfer catalyst, tetraoctylammonium bromide (TOAB), owing to the ion-pair adduct formation between silver nanoparticle anions and tetraoctylammonium cations. Smaller nanoparticles were found to be more readily transferred to the organic phase compared to larger nanoparticles. Various concentrations of TOAB in the organic elution phase were used in the CCC extraction experiments. It appeared that a concentration of 0.02 mM of TOAB was adequate to achieve optimum separation and recovery for the aqueous Ag nanoparticle sample (1.5 mg) in the CCC extraction experiments. Samples of 15.8 ± 5.3 nm were separated; the distributions of four fractions collected were 13.7 ± 1.9, 14.1 ± 3.5, 19.2 ± 4.3, and 22.2 ± 4.9 nm. Compared with the stepwise extraction performed in this study, the step-gradient extractions using CCC provided much better size discrimination.



## 1. Introduction

In the last decade, many separation techniques, including size exclusion chromatography [1,2], ion-pair chromatography [3], field-flow fractionation [4], gel electrophoresis [5,6], and diafiltration [7], have been developed for the size separation of nanoparticles. Ito et al. [8,9] demonstrated particle and cell separations using counter-current chromatography (CCC) in a non-synchronous coil planet centrifuge. Moreover, Fedotov [10] successfully fractionated micro-size particles suspended in single phase CCC using J type synchronous coil planet centrifuge. However, size separation of nanoparticles has not been reported using CCC. CCC is known as a support-free liquid–liquid chromatography [11,12], where irreversible adsorption would not occur. Accordingly, CCC is often applied in purifying crude extracts of natural products before regular HPLC/MS analysis [13,14]. In a typical CCC separation, a solvent system is made by mixing two or more solvents in a separatory funnel. After settling, two separate liquid layers (the upper and the lower phases) are formed. One of the two layers acts as the stationary phase and the other one is the mobile phase. Sample molecules are distributed in these two phases and separated during the elution. Typically, one of the phases is rich in water, i.e. hydrophilic; and the other one is rich in organic solvent, i.e. hydrophobic. However, water-dispersed nanoparticles are insoluble in hydrophobic media; thus, modifications of the solvent system are needed to adjust the partition between the two phases.

Hydrophobic surfactant, such as bis(2-ethylhexyl) sulfosuccinate (AOT) has often been applied as the stabilizing agent in the synthesis of metal nanoparticles in organic solvents [15,16]. Reverse micelles formed by AOT aggregates provide hydrophilic environments for nanoparticles. In addition, surfactant tetraoctylammonium bromide (TOAB) is a common cationic agent for phase transfer in nanotechnology. For example, $HAuCl_4$ can be transferred from water to toluene in the presence of TOAB and reduced to yield gold nanoparticles also stabilized by the surrounding TOAB molecules in toluene [17]. In addition to being a transfer agent for precursors and a stabilizing agent for nanoparticles, TOAB demonstrated extraction ability for noble metal nanoparticles that were modified by carboxyl groups possessing highly negative charges. The surfaces of gold or silver nanoparticles were usually capped by a monolayer of thiol molecules with Au–S, or Ag–S covalent binding. Thiol compounds, such as 11-mercaptoundecanoic acid (MUA) and mercaptosuccinic acid, were easily immobilized on gold and silver nanoparticles [18,19]. The extraction was attained through ion-pair formation between tetraoctylammonium cations ($TOA^+$) and the carboxyl group on nanoparticle surfaces [20]. Without TOAB, nanoparticles in the aqueous solution would not be transferred to toluene. With a low concentration of TOAB, relatively small-sized particles in the aqueous solution could be transferred more easily to the toluene. After the amount of small-sized particles

* Corresponding author. Tel.: +886 3 573 1673; fax: +886 3 572 3764.
*E-mail address:* tyu@faculty.nctu.edu.tw (T. Yu).

0021-9673/$ – see front matter © 2009 Elsevier B.V. All rights reserved.
doi:10.1016/j.chroma.2009.06.002

decreased owing to the first extraction, more relatively large-sized particles would readily move to the organic layer during the second extraction. Therefore, size separation could be performed by stepwise extractions using the organic solvents with the same TOAB concentration. In addition to the concentration of phase transfer agent, organic solvents used as the extraction media played an important role on the phase transfer. Chloroform and carbon tetrachloride exhibited higher extraction efficiency for larger particles than toluene [21]. Thus, size-selective extraction of silver nanoparticles could be achieved using a series of different organic solvents containing the same surfactant.

In addition to chromatographic separations, CCC was used as a continuous extractor, for example, in removing surfactants from waste water [22]. The scale-up of dynamic extraction has been demonstrated and improved through the modification of CCC centrifuges [23]. The phase distribution in a CCC column used as a continuous extraction vessel has been studied recently in order to enhance extraction efficiency [24]. In the present study, size-separation of Ag nanoparticles using CCC was performed with solvent systems containing TOAB. Solutes dissolved in the aqueous stationary phase were eluted with the organic mobile phase. Although the extraction signal monitored using an on-line detector looked a little similar to chromatograms, the separation was achieved through a batch extraction process of Ag nanoparticles using a step-gradient of TOAB in the mobile phase.

## 2. Experimental

### 2.1. Reagents and solvents

HPLC-grade *n*-hexane and toluene were purchased from Tedia (Fairfield, OH, USA). Sodium borohydride, TOAB, and MUA were all purchased from Sigma–Aldrich (St. Louis, MO, USA). Silver nitrate, hydrochloric acid, potassium dihydrogenphosphate ($KH_2PO_4$), and dipotassium phosphate ($K_2HPO_4$) were obtained from Showa (Tokyo, Japan). Water was purified using a Milli-Q apparatus (Millipore, Bedford, MA, USA).

### 2.2. Preparation of aqueous Ag nanoparticles

Silver nanoparticles modified by MUA (Ag-MUA) were prepared using the method similar to the steps reported in the literature [18]. At the beginning, 1.7 mg of MUA was added into 25 ml of freshly prepared sodium borohydride aqueous solution (20 mM). After stirring for 5 min, 25 ml of silver nitrate solution (5 mM) was added by drops into the aqueous solution with vigorous stirring. The color of the clear solution turned to light yellow at first and finally to dark yellow due to the formation of silver nanoparticles. After 24 h of stirring, the solution was adjusted to pH 2 by adding 0.1 M HCl and the nanoparticles was precipitated by a centrifuge (Hermle Z323K centrifuge, Wehingen, Germany) running under 6000 rpm for 10 min. The precipitate (15 mg) was re-dispersed in 50 ml of phosphate buffer (20 mM, pH 11) as the stock solution. Because aggregates of silver nanoparticles would be enhanced by higher salt concentration [25], the phosphate buffer used in this experiment should be limited to 20 mM.

### 2.3. Analysis of Ag nanoparticles

#### 2.3.1. Optical spectroscopy

The Ag-MUA stock solution (0.30 mg/ml) was diluted 30 times (owing to the high absorptivity) with deionized water to be characterized using a UV–vis spectrophotometer (Hewlett-Packard 8453, Waldbronn, Germany). In addition to the measurement of Ag-MUA in the aqueous solution, Ag-MUA in an organic solvent was also investigated. Phase transfer was also operated by mixing 10 ml of the stock solution with 10 ml of 1 mM TOAB-containing toluene/hexane (1:1, v/v) solution for 20 min. The upper organic phase was diluted 15 times with the hexane/toluene mixture and was measured with the UV–vis spectrophotometer.

To identify the functional groups on the surface of nanoparticles, a KBr pellet of the Ag-MUA powder dried under vacuum was made for measuring IR spectrum using a Bio-Rad FTS 165 infrared spectrophotometer (Philadelphia, PA, USA). A KBr pellet of the MUA powder was made to provide a blank measurement.

#### 2.3.2. Electron microscopy

The synthesized Ag-MUA was diluted 100-fold by water and a small drop was tipped on a glass substrate and dried under vacuum. The substrate was sputtered to form a 2 nm platinum thin film in order to enhance the image resolution. The diameters of Ag-MUA were measured by a JEOL JSM-7401F (Tokyo, Japan) field emission scanning electron microscopy (SEM) system. The collected Ag-MUA nanoparticles from stepwise extraction and the CCC separations were also examined using the same instrument. In addition, the energy dispersive X-ray (EDX) spectrum was measured for the elements C, O, Ag, and S at the acceleration voltage of 10 keV.

### 2.4. Batch extraction using CCC instrument

The chromatograph used was a Model CCC-1000 (Pharma-Tech Research, MD, USA) high-speed CCC that was mounted in a temperature-controlled oven. It contained three spool-shape column holders; only one holder was used which was coiled with a 19-m long, 1.6-mm I.D. polytetrafluoroethylene (PTFE) tubing, with a total volume of 38 ml.

The coil was first filled with hexane/toluene (1:1, v/v) mobile phase solution without TOAB. The Ag-MUA stock solution prepared for the analytical purpose was also used as the sample solution for separation. The sample solution dispersed in phosphate buffer (20 mM, pH 11) was injected through a six-port injection valve with a coil of 5 ml into the tail end of the column. The rotation of the chromatograph was set at 700 rpm and the oven temperature was controlled at 20 °C. After sample loading, the extraction solution (TOAB-containing organic phase) was then pumped in using the tail-to-head mode. Flow rate was 1 ml/min for all experiments. The mobile phases were mixtures of hexane/toluene (1:1, v/v) containing various concentrations (0.1, 0.03, 0.02, and 0.01 mM) of TOAB. The effluent was monitored using a Bio-Rad Model 1801UV detector (Hercules, CA, USA) at 427 nm, and every 2 ml was collected using an Advantec CHF 121SA fraction collector (Tokyo, Japan).

### 2.5. Stepwise extraction of Ag-MUA nanoparticles

The aqueous solution of 1.5 mg Ag-MUA dispersed in 5 ml phosphate buffer (20 mM, pH 11) was mixed with the organic solution of 10 ml TOAB (0.02 mM)-containing hexane/toluene (1:1, v/v). After vigorous stirring for 20 min, the upper phase was removed and another fresh 10 ml organic phase was added for the second extraction. The process was repeated four times and the extracted portions were analyzed by SEM for the size distribution.

## 3. Results and discussion

### 3.1. Characterizations of Ag-MUA nanoparticles

The UV–vis spectra of the silver nanoparticles are shown in Fig. 1. The Ag-MUA nanoparticles in aqueous solution gave a maximum wavelength of surface plasmon resonance absorbance at 416 nm. In the absence of TOAB, mixing of the Ag-MUA aqueous phase with the hexane/toluene phase did not result in the successful transfer of

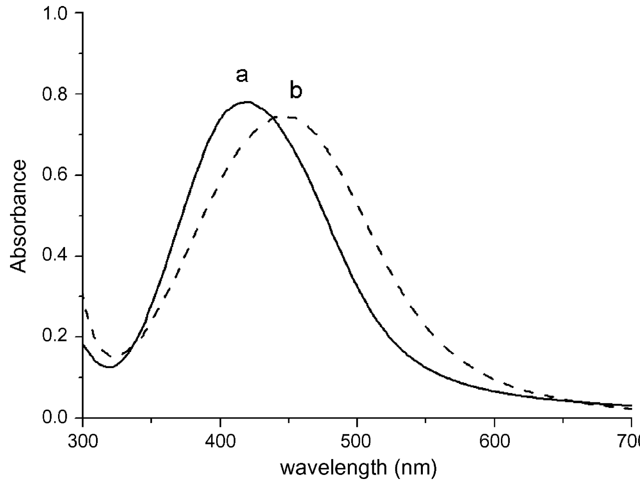


**Fig. 1.** UV–vis spectra of Ag-MUA nanoparticles in aqueous solution (a) and after extraction to hexane/toluene (b).

the Ag-MUA to the organic phase. The organic layer remained colorless after thorough mixing and showed no UV–vis absorbance at 416 nm. To estimate the amount of MUA molecules, elemental analyses of the sample using EDX were conducted to estimate the atomic percentage. The average S/Ag ratio was ∼0.07 and the weight fraction of MUA molecule was about 12.4 wt%. After eliminating impurities and $H_2O$ molecules combined with the carbonyl groups [26], the calculated amount of MUA in the sample for the UV–vis absorbance measurement was ∼1.5 μmole. Compared with the TOAB (10 μmole) in the organic phase, a quantitative transfer was thus observed using UV–vis absorbance measurement.

The organic layer turned into dark yellow after 20-min stirring while the aqueous layer became colorless. The maximum absorbance of organic layer appeared at 446 nm. An 30-nm red shift in the surface plasmon resonance absorbance was observed. Red shifts were also observed from 4 to 22 nm, while gold nanoparticles were transferred from the aqueous to the organic phase [27]. Therefore, the red shifts in the present experiment might have resulted from the change in the refractive index of the Ag-MUA nanoparticles. The IR spectra of the Ag-MUA nanoparticles and pure MUA are shown in Fig. 2. The FTIR spectra of Ag-MUA nanoparticles showed significant vibration peaks of carboxylic acid stretching (1740 $cm^{-1}$) [28] and CH stretching (2917, 2852 $cm^{-1}$). It was noted that the S–H

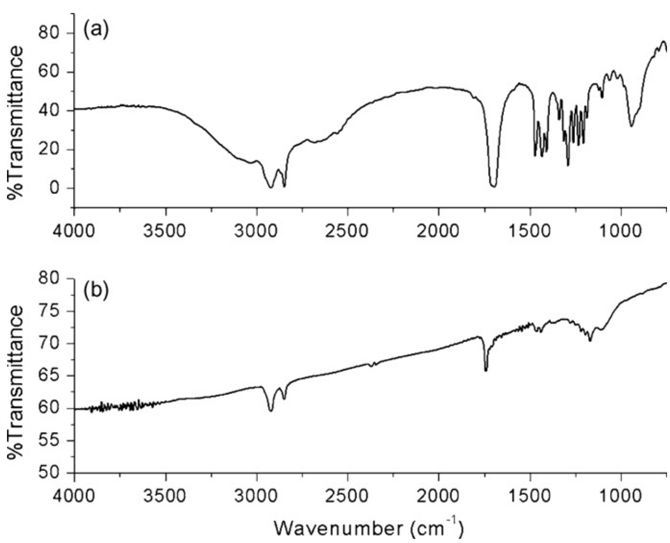


**Fig. 2.** FT-IR spectra of the MUA molecules (a) and Ag-MUA powder (b).

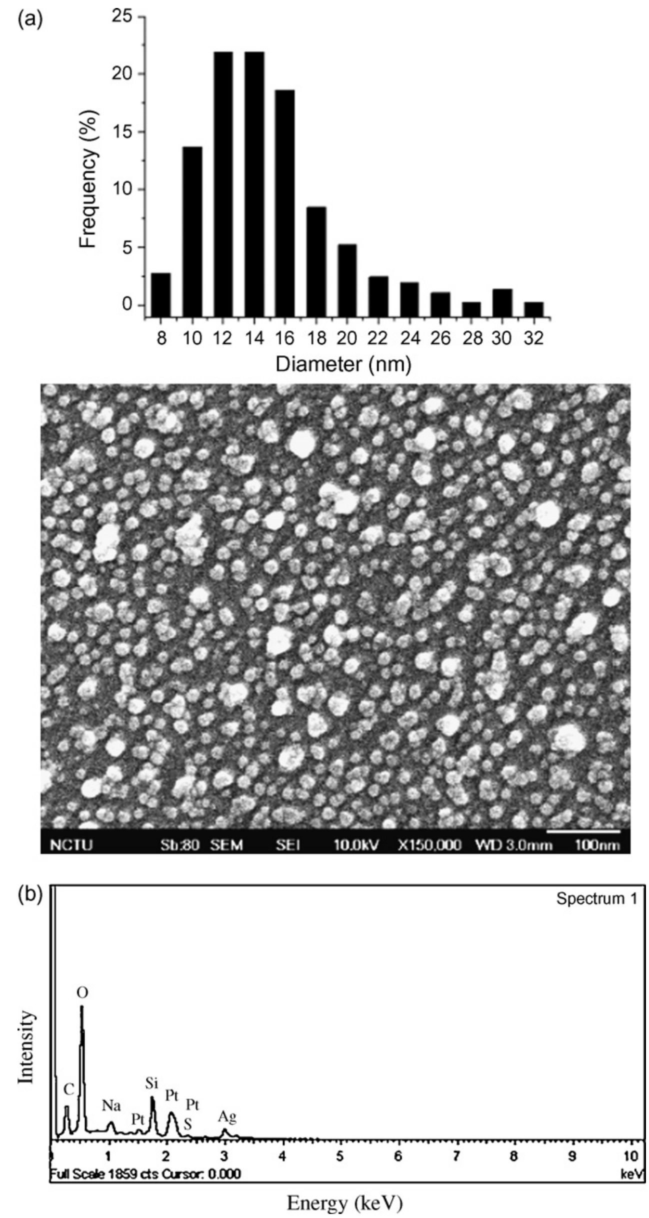


**Fig. 3.** (a) Size distribution and SEM image of the Ag-MUA nanoparticles and (b) EDX spectrum of the Ag-MUA nanoparticles.

stretching signal (2550–2600 $cm^{-1}$) shown on the MUA IR spectrum was absent in the Ag-MUA sample. This suggested that the S–H stretch of the MUA molecule would have been eliminated and replaced by Ag–S formation [18]. The particle size distributions of 300 nanoparticles were measured using SEM and the images are shown in Fig. 3a. The average diameter and standard deviation of nanoparticles were 15.8 ± 5.3 nm. The EDX spectrum for C, Ag, O, S, Si, and Pt is shown in Fig. 3b. The Si and Pt signals emerged from the glass substrate and the Pt sputtering. The unusually high intensity of O might also result from the glass substrate in addition to the COOH moiety of the MUA molecule.

### *3.2. Size-fractionation of Ag-MUA nanoparticles using CCC*

At the beginning of the study, we tried to find a conventional aqueous-organic solvent system that might provide adequate partition coefficient for different sizes of Ag-MUA nanoparticles. Because the p$K_a$ of monolayer MUA self-assembled on the metal surface was 5.7 under 0.1 M ionic strength and was 4.4 under higher ionic strength [29], the Ag-MUA nanoparticles in aqueous phase were very hydrophilic, while the pH was above 6. No detectable Ag-MUA particles were found transferred to the hexane/toluene phase. The pH of the aqueous layer was then lowered to increase the hydrophobicity of the particles. Unfortunately, no partition of Ag-MUA was observed even when the pH was adjusted to below 2. Instead of moving into the organic layer, precipitate of Ag-MUA formed at the water–hexane/toluene interface. Under higher pH values, Ag-MUA nanoparticles were subjected to greater electrostatic repulsion and were dispersed well in the aqueous layer and prevented from aggregation. Accordingly, surfactant TOAB was added to the organic layer to promote the Ag-MUA partition into the organic layer.

The partitions of Ag-MUA between the aqueous and TOAB-containing hexane/toluene solutions were examined. With the presence of TOAB, ion-pair adduct [Ag-MUA$^{n-}$·$n$TOA$^+$] would form between MUA anions and TOA$^+$ cations [20] after mixing. This adduct was insoluble in water, thus once it entered the organic phase during the mixing, it would not return to the aqueous phase. In the mean time, phosphate anions might also move into the organic phase due to the ion-pair formation. However, the Ag-MUA should be transferred into the organic phase more favorably than phosphate anions due to the hydrophobic interaction between the long alky-chains of Ag-MUA and TOAB. Therefore, a partition CCC was not feasible in this application. If the solvent system was prepared in the conventional way by mutual saturation of the aqueous and the organic portions, the Ag-MUA particles would move into the organic mobile phase quantitatively during the elution without size separation. Accordingly, a batch extraction was performed, as described in Section 2.4, using the TOAB-containing organic phase, instead of a conventional partition CCC.

The Ag-MUA extraction signals and the fraction collection times are given in Fig. 4. Only one large peak, shown in Fig. 4a, was obtained at ~50 min by elution of the extraction liquid containing 0.1 mM TOAB. This could have resulted from the high concentration of TOAB in the organic phase. Since the sample contained only 0.75 μmole MUA, most Ag-MUA particles were transferred into the organic mobile phase of ~25 ml (equivalent to 2.5 μmole TOAB) in the dynamic process. All Ag-MUA particles with different diameters were transferred from the aqueous phase to the organic phase at the same time. Consequently, only a single peak appeared almost at the solvent front.

The TOAB concentration was then reduced in the following experiments to facilitate better size discrimination. An extraction peak with a shoulder, shown in Fig. 4b, was observed by eluting with a 0.03 mM TOAB solution. Furthermore, two even lower TOAB concentrations (0.02 and 0.01 mM) were studied. The extraction signals extended to a much greater range as the concentration was lowered. This occurred because of the lower solvation power (less ion-pair formation) of the lower concentration. While extraction solutions of higher TOAB concentrations carried more Ag-MUA particles into the organic phase with less extraction volume, those of lower TOAB concentrations took longer time (more elution volume) to bring all particles into the organic phase, thus could give better size discrimination.

The size distributions of the collected fractions for all four experiments measured by SEM are listed in Table 1. The average diameters in the four portions showed no significant difference in the elution using 0.1 mM TOAB. In fact, the distributions (~16.0 nm) of these fractions were similar to those of the original samples. Only the deviations of the fractions became greater when collected at the longer elution time. When the extraction solvent front just arrived at the sample zone, small-sized particles were still favored

**Table 1**
Size distributions of nanoparticles for the fractions of the continuous extractions and the stepwise extraction (synthesized sample = 15.8 ± 5.3 nm).

| | Fraction 1 | Fraction 2 | Fraction 3 | Fraction 4 |
|---|---|---|---|---|
| a | 15.6 ± 3.1 nm | 16.0 ± 3.5 nm | 15.9 ± 4.0 nm | 16.1 ± 4.2 nm |
| b | 13.8 ± 2.5 nm | 15.4 ± 3.3 nm | 16.2 ± 4.1 nm | 19.2 ± 5.0 nm |
| c | 13.7 ± 1.9 nm | 14.1 ± 3.5 nm | 19.2 ± 4.3 nm | 22.2 ± 4.9 nm |
| d | 13.1 ± 2.3 nm | 14.5 ± 2.6 nm | 15.2 ± 3.5 nm | 15.5 ± 4.2 nm |
| e | 14.2 ± 3.0 nm | 15.1 ± 3.3 nm | 15.9 ± 4.1 nm | 17.5 ± 4.4 nm |

a. Continuous extraction using 0.1 mM TOAB solution.
b. Continuous extraction using 0.03 mM TOAB solution.
c. Continuous extraction using 0.02 mM TOAB solution.
d. Continuous extraction using 0.01 mM TOAB solution.
e. Stepwise extraction using 0.02 mM TOAB solution.

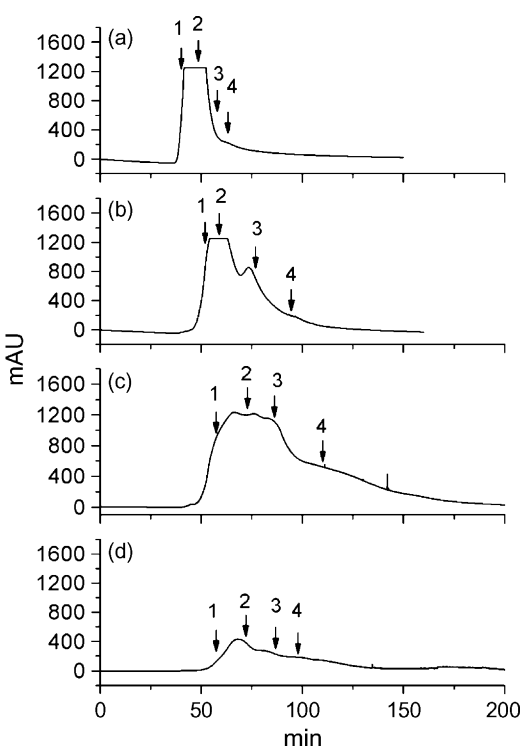


**Fig. 4.** Batch step-gradient extraction experiments of Ag-MUA nanoparticles using the solvents of 0.1 mM (a), 0.03 mM (b), 0.02 mM (c), and 0.01 mM (d) TOAB in hexane/toluene (1:1, v/v). The starting collection times (marked by arrows) for the four fractions were 42, 50, 58, and 62 min for (a); 58, 62, 78, and 90 min for (b); 60, 74, 88, and 110 min for (c) and 60, 74, 88, and 90 min for (d).

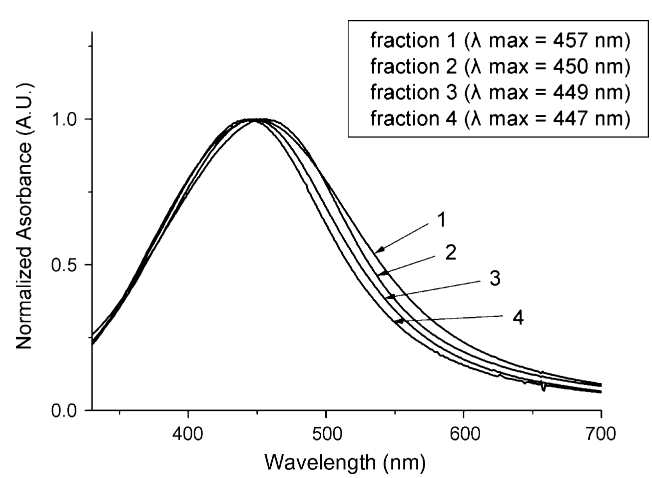


**Fig. 5.** UV–visible absorption spectra of silver nanoparticles collected fractions during the CCC process (0.02 mM TOAB). The spectra were normalized by the maxima of each peak. Blue shifts were found in the collection order.

to enter the elution solvent, thus resulting in a narrow distribution in the first fraction. As more solvent was delivered into the column, larger-sized particles also started moving into the elution solvent, thus resulted in greater deviation but without size selectivity. No fractions were collected after 75 min owing to the negligible signal amplitude.

The four fractions of the second experiment, shown in Fig. 4b, were collected across the two unresolved peaks and at the peak tail. The size distributions changed more significantly from 13.8 to 19.2 nm along with the elution time. Apparently, the size discrimination was improved through lower TOAB concentration. While using 0.02 mM TOAB, the extraction signal, Fig. 4c, showed an irregular broad band and extended tailing to ∼200 min. The average size became broader for the four fractions collected under the large peak. When the TOAB concentration was further reduced to 0.01 mM, the elution signal intensity became significantly reduced with a tailing peak recorded at ∼62 min (Fig. 4d). When the elution was completed, the liquid in CCC was purged using nitrogen gas. Some black precipitates appeared in the water–organic interface and on the inner surface of the PTFE tubing, probably because of nanoparticle aggregation. The extraction phase might not provide enough solvent power for the charged nanoparticles and the water-dispersion ability of nanoparticle might be spoiled, thus forming particle aggregates. The relatively small average sizes for the collected fractions, listed in Table 1, also reflected the low intensity of the on-line signal. Large-sized particles remained in the column without being extracted and formed aggregates.

Extraction using 0.02 mM TOAB gave the best result among the four experiments. The collected four fractions were measured using the UV–vis spectrophotometer and the normalized absorbance spectra are shown in Fig. 5. Blue shifts (10–20 nm) were observed. It indicated increasing particle size in the order of collected fractions [30,31]. The SEM images and particle size distribution of the four fractions under this experiment are shown in Fig. 6. Basi-

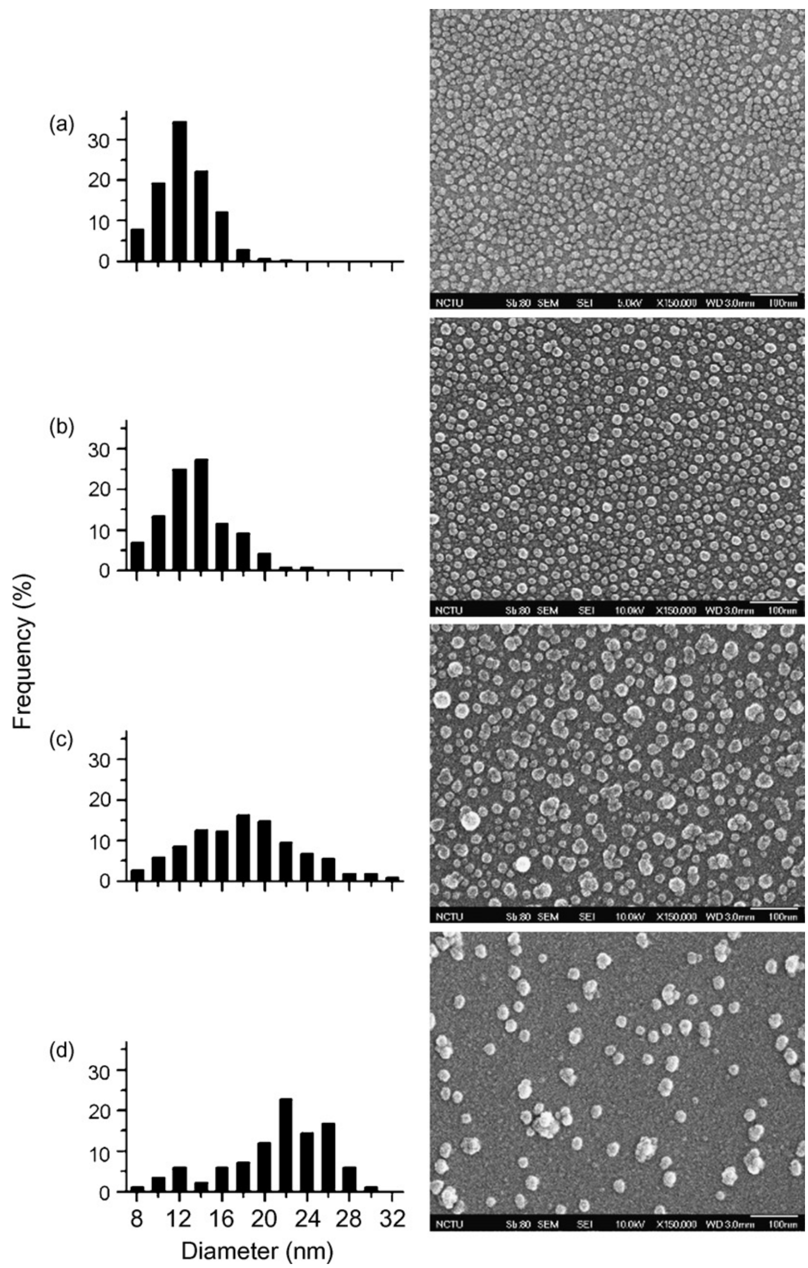


**Fig. 6.** Particle size distributions and the SEM images of fraction 1 (a), fraction 2 (b), fraction 3 (c), and fraction 4 (d) for the batch step-gradient extraction using 0.02 mM TOAB.

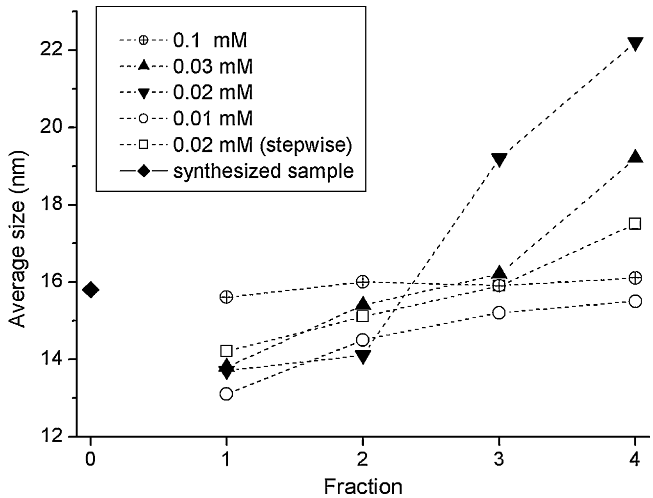


**Fig. 7.** Particle size distributions (without standard deviations) for the fractions of the batch step-gradient extractions and the fractions of the stepwise extraction.

cally, the average size became greater as the elution time increased. In the first fraction, the average diameter 13.7 nm was smaller than that of the synthesized 15.8 nm sample and the standard deviation 1.9 nm was also appreciably smaller than the 5.3 nm sample. The particle images revealed a relatively uniform distribution. The size distribution of the second portion appeared similar to that of the first portion. Size discrimination was not very pronounced between these two portions. The third portion collected at the right edge of the broad peak, shown in Fig. 4c, gave a much broader distribution (standard deviation 4.3 nm) with the average size of 19.2 nm. The proportion of the smaller size particles had been greatly reduced in this fraction considering the population of small particles (≦18 nm) that dominated in the original sample. The fourth fraction (22.2 ± 4.9 nm) further reflected this trend. Smaller particles had been removed to a large extent in the previous three collections. While large particles further dominated in this portion, those very large particles (>30 nm) were, on the contrary, reduced to an undetectable level. Those very large particles might have been already eliminated during the early extraction stages.

### 3.3. Size-fractionation of Ag-MUA nanoparticles using stepwise extractions

A stepwise extraction was also carried out using the 0.02 mM TOAB solution for comparison. It was assumed that TOAB molecules were paired with MUA molecules on the Ag-MUA particles by 1:1 ratio. The total amount of MUA molecules on the nanoparticle surfaces could not exceed the number of moles (0.75 μmole) added for synthesis. By calculation, extraction volume 39 ml of 0.02 mM TOAB (equivalent to 0.78 μmole) solution was more than enough to transport all Ag-MUA particles from the sample solution to the organic phase. Accordingly, a four-step extraction was operated with 10 ml organic phase for each step. The size distributions are listed in Table 1. In addition, particle size distributions of the batch step-gradient and the stepwise extractions are illustrated in Fig. 7. The stepwise extraction appeared to prevail compared with the batch step-gradient extractions using 0.1 and 0.01 mM, i.e. the highest and lowest TOAB concentrations. Surfactant concentration obviously played a very important role in size discrimination, as stated before. As for the batch step-gradient extraction using 0.03 mM, the isolation of large particles became better than that of the stepwise process. The fourth portion of this batch step-gradient extraction gave a value of 19.2 ± 5.0 nm contrasted with 17.5 ± 4.2 nm of the stepwise process. Under the same TOAB concentration (0.02 mM), the batch step-gradient extraction showed much better size discrimination than either the stepwise extraction or other batch step-gradient extractions. Especially, the average sizes of the third and the fourth fractions shifted to 19.2 and 22.2 nm, which were significantly greater than those of all other extractions.

## 4. Conclusions

We employed surfactant-containing organic solvent using CCC to separate the sizes of the Ag-nanoparticle samples. The CCC column can be considered as a batch multi-stage extraction system using a step-gradient of TOAB in the mobile phase to enhance efficiency. The concentration of the surfactant TOAB in this dynamic extraction controlled the size distribution of the collected fractions. This study showed the viability of improving the size discrimination of using surfactant-containing solvent for nanoparticle separation.

## Acknowledgment

The authors would like to thank the National Science Council of Taiwan for their financial support (NSC 96-2113-M-009-024).

## References

[1] G.T. Wei, F.K. Liu, C.R.C. Wang, Anal. Chem. 71 (1999) 2085.
[2] J.P. Novak, C. Nickerson, S. Franzen, D.L. Feldheim, Anal. Chem. 73 (2001) 5758.
[3] M.M.F. Choi, A.D. Douglas, R.W. Murray, Anal. Chem. 78 (2006) 2779.
[4] A.H. Latham, R.S. Freitas, P. Schiffer, M.E. Williams, Anal. Chem. 77 (2005) 5055.
[5] X.Y. Xu, K.K. Caswell, E. Tucker, S. Kabisatpathy, K.L. Brodhacker, W.A. Scrivens, J. Chromatogr. A 1167 (2007) 35.
[6] M. Hanauer, S. Pierrat, I. Zins, A. Lotz, C. Sonnichsen, Nano Lett. 7 (2007) 2881.
[7] S.F. Sweeney, G.H. Woehrle, J.E. Hutchison, J. Am. Chem. Soc. 128 (2006) 3190.
[8] Y. Ito, M. Weinstein, T. Aoki, R. Harada, E. Kimura, K. Nunogaki, Nature 212 (1966) 985.
[9] Y. Ito, P. Carmeci, I.A. Sutherland, Anal. Biochem. 94 (1979) 249.
[10] P.S. Fedotov, J. Liq. Chromatogr. Relat. Technol. 25 (2002) 2065.
[11] Y. Ito, W.D. Conway, High-Speed Countercurrent Chromatography, Wiley, 1996.
[12] Y. Ito, R.L. Bowman, Anal. Biochem. 82 (1977) 63.
[13] A. Weisz, Y. Ito, J. Chromatogr. A 1198 (2008) 232.
[14] G. Jerz, T. Skotzki, K. Fiege, P. Winterhalter, S. Wybraniec, J. Chromatogr. A 1190 (2008) 63.
[15] C. Petit, P. Lixon, M.P. Pileni, J. Phys. Chem. 97 (1993) 12974.
[16] B.L.V. Prasad, S.K. Arumugarn, T. Bala, M. Sastry, Langmuir 21 (2005) 822.
[17] M. Brust, M. Walker, D. Bethell, D.J. Schiffrin, R. Whyman, J. Chem. Soc., Chem. Commun. (1994) 801.
[18] W.L. Shi, Y. Sahoo, M.T. Swihart, Colloids Surf. A 246 (2004) 109.
[19] T. Huang, P.D. Nallathamby, D. Gillet, X.H.N. Xu, Anal. Chem. 79 (2007) 7708.
[20] H. Yao, O. Momozawa, T. Hamatani, K. Kimura, Chem. Mater. 13 (2001) 4692.
[21] Y. Yang, K. Kimura, Chem. Lett. 35 (2006) 462.
[22] A. Berthod, Encyclopedia of Environmental Analysis and Remediation, Wiley, 1998.
[23] I.A. Sutherland, J. Chromatogr. A 1151 (2007) 6.
[24] R. van den Heuvel, I.A. Sutherland, J. Chromatogr. A 1216 (2009) 4252.
[25] K. Das, A. Uppal, P.K. Gupta, Chem. Phys. Lett. 426 (2006) 155.
[26] S.H. Chen, K. Kimura, Langmuir 15 (1999) 1075.
[27] W.L. Cheng, E. Wang, J. Phys. Chem. B 108 (2004) 24.
[28] B.L. Frey, R.M. Corn, Anal. Chem. 68 (1996) 3187.
[29] J.F. Smalley, K. Chalfant, S.W. Feldberg, T.M. Nahir, E.F. Bowden, J. Phys. Chem. B 103 (1999) 1676.
[30] A. Taleb, C. Petit, M.P. Pileni, Chem. Mater. 9 (1997) 950.
[31] J.P. Wilcoxon, J.E. Martin, P. Provencio, J. Chem. Phys. 115 (2001) 998.